Editorial Manager(tm) for Journal of Electronic Materials
Manuscript Draft

Manuscript Number: JEMS-1377

Title: Self-Assembled Germanium Quantum-Dot Supercrystals in Silicon with Extremely Low Thermal Conductivities

Article Type: S.I.: ICT2009

Keywords: Thermoelectrics, Thermal Conductivity, Self-Assembly, Quantum Dot, Silicon, Germanium

Corresponding Author: Jean-Numa Gillet,

Corresponding Author's Institution: University of Lille 1

First Author: Jean-Numa Gillet, Ph.D.

Order of Authors: Jean-Numa Gillet, Ph.D.; Sebastian Volz, Ph.D.

Self-Assembled Germanium Quantum-Dot Supercrystals in Silicon with Extremely Low Thermal Conductivities

Jean-Numa Gillet,[1,*] Sebastian Volz[2]

[1] Institut d'Electronique, de Microélectronique et de Nanotechnologie (IEMN, CNRS UMR 8520), Dept. of Physics, Université de Lille 1, Av. Poincaré, BP 60069, 59652 Villeneuve d'Ascq Cedex, France
[2] Laboratoire d'Energétique Moléculaire et Macroscopique (EM2C, CNRS UPR 288), Ecole Centrale Paris, Grande Voie des Vignes, 92295 Châtenay-Malabry Cedex, France
*Corresponding author's email: jean-numa.gillet@univ-lille1.fr

ABSTRACT

One-dimensional (1D) superlattices with a low thermal conductivity were studied for thermoelectrics. Since they are composed of materials with a lattice mismatch, they often show dislocations. It is therefore challenging to fabricate superlattices with a thermoelectric figure of merit *ZT* higher than unity. Like 1D nanowires, they also decrease heat transport in only one main direction. Epitaxial self-assembly is a major technology to fabricate three-dimensional (3D) Ge quantum-dot (QD) arrays in Si. They were used for quantum and solar-energy devices. Using the atomic-scale phononic crystal model, 3D Ge QD supercrystals in Si can also present an extreme reduction of the thermal conductivity with an ultra-low value as tiny as 0.04 W/m/K. Owing to incoherent phonon scattering, the same conclusion holds for 3D supercrystals with moderate QD disordering. As a result, they might be considered to design highly-efficient CMOS-compatible thermoelectric devices with *ZT* possibly much higher than unity. A so small thermal conductivity was only obtained for two-dimensional layered WSe_2 crystals in an experimental study. However, electronic conduction in the Si/Ge compounds is significantly enhanced. The 0.04 W/m/K value can be computed for different Ge-QD filling ratios of the Si/Ge supercrystal with size parameters in the range of current fabrication technologies.

Keywords: Thermoelectrics, Thermal Conductivity, Self-Assembly, Quantum Dot, Silicon, Germanium
(Submitted to J. Electronic Materials in the frame of the special issue of ICT 2009, Freiburg, DE)

I. INTRODUCTION

The Carnot energy-conversion efficiency η_c of a thermoelectric material is an increasing function of its thermoelectric figure of merit ZT that is inversely proportional to its thermal conductivity λ. However, λ is directly proportional to its power factor ($S^2\sigma$). In fact, when S, σ and T denote the Seebeck coefficient, electrical conductivity and absolute temperature, respectively, the non-dimensional ZT is given by $ZT = S^2\sigma T/\lambda$ [1,2]. The discovery of a material with ZT higher than 2-3 yields η_c higher than 50 %, which could have an enormous impact for energy conversion and renewable energies. As a consequence, the design of semiconducting materials with an indirect electronic bandgap showing a very low thermal conductivity is currently one of the major areas of research in solid-state physics and chemistry [1-10].

One-dimensional (1D) superlattices with periodic thin semiconducting layers were the first type of nanomaterials to be studied in the purpose of achieving $ZT > 1$. The thermal conductivity of a 1D superlattice can be significantly reduced compared with a bulk material due to phonon confinement between its layer interfaces [6,9]. However, the design of a material with ZT larger than unity is usually not possible with the superlattices. In fact, the lattice mismatch at their layer interfaces forms dislocations that often lead to cracks owing to high residual stresses from the covalent bonds stopping dislocation propagation. These defects lead to σ reduction and avoid ZT increase with respect to unity. Recently, 1D nanowires were also proposed for thermal conductivity reduction [3-5]. Nevertheless, like 1D superlattices, they decrease thermal transport in only one main direction. Therefore phonon confinement, as non-focusing and localization, cannot be as significant as in three-dimensional (3D) nanomaterials. Experimentally, these 1D materials usually fail to beat the lowest amorphous limit of bulk Si around 1 W/m/K [10].

With the spectacular development of nanotechnology, self-assembly became a major technology for bottom-up fabrication of 3D nanostructured devices for various applications in drug design, biotechnologies, electronics, photonics, etc. Self-assembly of epitaxial layers on silicon has been used to fabricate 3D Ge quantum-dot (QD) arrays in diamond-cubic (dc) Si for quantum-device and solar-energy applications. In this theoretical study, we show - from the atomic-scale 3D phononic crystal model [11] - that high-density 3D arrays of self-assembled (SA) Ge QDs surrounded by a dc Si matrix can also present an extreme reduction of the thermal conductivity with an ultra-low value can be as tiny as 0.04 W/m/K at room temperature (less than twice that of air). This quantity represents a 3750-fold reduction factor with respect to bulk dc Si (150 W/m/K). As a result, these 3D Si/Ge QD supercrystals, with double-scale crystallinity, could be considered to design very efficient thermoelectric devices showing compatibility with CMOS microelectronics. A thermal conductivity with a similar value of 0.05 W/m/K was obtained in a preceding experimental study of two-dimensional (2D) disordered layered WSe_2 crystals [6]. This value also shows a significant reduction with respect to the extreme low limit of amorphous WSe_2 of the order of 0.3 W/m/K [6,12]. However, electronic transport in the Si/Ge crystals can be significantly enhanced compared with the WSe_2 crystals by electrical doping using conventional CMOS processes. Moreover, WSe_2 is a toxic compound for living organisms.

The phonon harmonic behavior in the atomic-scale 3D phononic crystal is modeled from its dispersion curves that are computed in the THz range by lattice dynamics [13-15]. Flat dispersion curves with mini bandgaps are obtained for the higher-energy folded modes. This phenomenon leads to much smaller phonon group velocities than those of bulk dc Si. The huge decrease of the thermal conductivity in the atomic-scale 3D phononic crystal is not only due to the harmonic effects of the low phonon group velocities. Additional incoherent effects of phonon multiple scattering between the Ge QDs have to be considered owing to a

wave-particle duality appearing when the folded phonon wavelengths are smaller than the double lattice constant 2*d* of the supercells in the Si/Ge QD supercrystal. Multiple scattering breaks the phonon mean free paths (MFPs) and constitutes another thermal-conductivity reduction factor in the QD supercrystal. Incoherent scattering can be modeled using a near-field theory as that from van de Hulst and other authors [16-18]. Owing to its predominance, strong non-focusing and localization effects of the phonons appear. Indeed, the density of thermal paths is low owing to double-scale crystallinity in the 3D Si/Ge QD supercrystal. Thus, the supercrystal thermal conductivity can be much lower than that of the lowest amorphous limits of related bulk materials like Si or WSe_2. In fact, the heat flux can find a larger number of random thermal paths in amorphous materials as experimentally obtained in Ref. [6]. From the precedent, the same extreme reduction of the thermal conductivity holds for 3D Si/Ge QD supercrystals if the degree of QD disordering remains moderate with respect to an amorphous Si/Ge material.

In first numerical results, we show for a wide temperature range that the thermal conductivity decreases for an increasing QD filling ratio *x* (in Ge at %) in the case of a supercell with a constant average distance *d* between the Ge QDs. In an atomic-scale 3D phononic crystal where each supercell is made up of a QD with 1332 Ge atoms inside a cage of 1412 Si atoms, the thermal conductivity can be decreased by a factor of 750 or more compared with bulk dc Si or below the upper limit of only 0.2 W/m/K. This value is 5 folds smaller than the Einstein limit around 1 W/mK of disordered bulk Si [12]. Thereafter, we present the size dependence of the thermal conductivity λ vs. the average distance *d* between the QDs. A λ decrease with a power law is observed for an increasing *d*. This analysis enables us to predict that λ can be as low as 0.04 W/m/K for two different QD filling ratios *x* (at room temperature). For instance, when *x* = 12.5 Ge at% or *x* = 48.5 Ge at%, the *d*-values to obtain the same λ = 0.04 W/m/K are 19.6 nm or 7.6 nm, respectively. These presented

numerical results might have a significant impact for thermoelectrics and forthcoming fabrication of a 3D Ge/Si supercrystal.

II. ATOMIC-SCALE 3D PHONONIC CRYSTAL MODEL

A. Confinement from Flat Dispersion Curves

To investigate the extreme thermal conductivity reduction of 3D high-density arrays of SA Ge QDs in a dc Si matrix, we propose the atomic-scale 3D phononic crystal model with a supercrystal lattice constant $d = Na$ given by an integer number of inter-atomic distances a in the <100> directions. As shown in Fig. 1, a period of this phononic-like crystal is made up of a group of $N \times N \times N = N^3$ dc Si cells. Therefore, the N^3 dc primitive cells form a larger cubic supercell in a simple-cubic (sc) supercrystal. When $N = 7$, as depicted in Fig. 1, each supercell is composed of $N^3 = 343$ dc primitive cells. In this example, the possible phononic-like crystals have a non-relaxed $d = Na = 7a = 3.8017$ nm, where $a = 0.5431$ nm is the lattice constant of bulk dc Si. The total number of atoms forming a supercell is $8N^3 = 2744$ since the number of atoms per primitive cubic cell is 8 in the dc subgroup. At each supercell center, we substitute a number of Si atoms by Ge atoms to obtain a 3D Ge/Si nanocomposite. In five possible atomic configurations with $N = 7$, we substitute the Si atoms contained in a subset of $M \times M \times M = M^3$ dc primitive cells, located at each supercell center, by Ge atoms to form Ge QDs (with a boxlike nanoparticle shape) with different bases $w = Ma$. The number of dc Ge inter-atomic distances is $M = 1$, 2, 3, 4 or 5 in the <100> symmetric directions.

When the size parameter M is equal to 1, 2, 3, 4 or 5, the central dc Ge QD in each supercell contains 28, 126, 344, 730 or 1332 Ge atoms, respectively. The latter atoms are surrounded by 2716, 2618, 2400, 2014 or 1412 Si atoms, respectively. The example with $M =$

5 refers to the largest QD basis $w = Ma = 5a = 2.7155$ nm among the defined 3D Si/Ge QD supercrystals with the supercrystal lattice constant $d = Na = 7a = 3.8017$ nm.

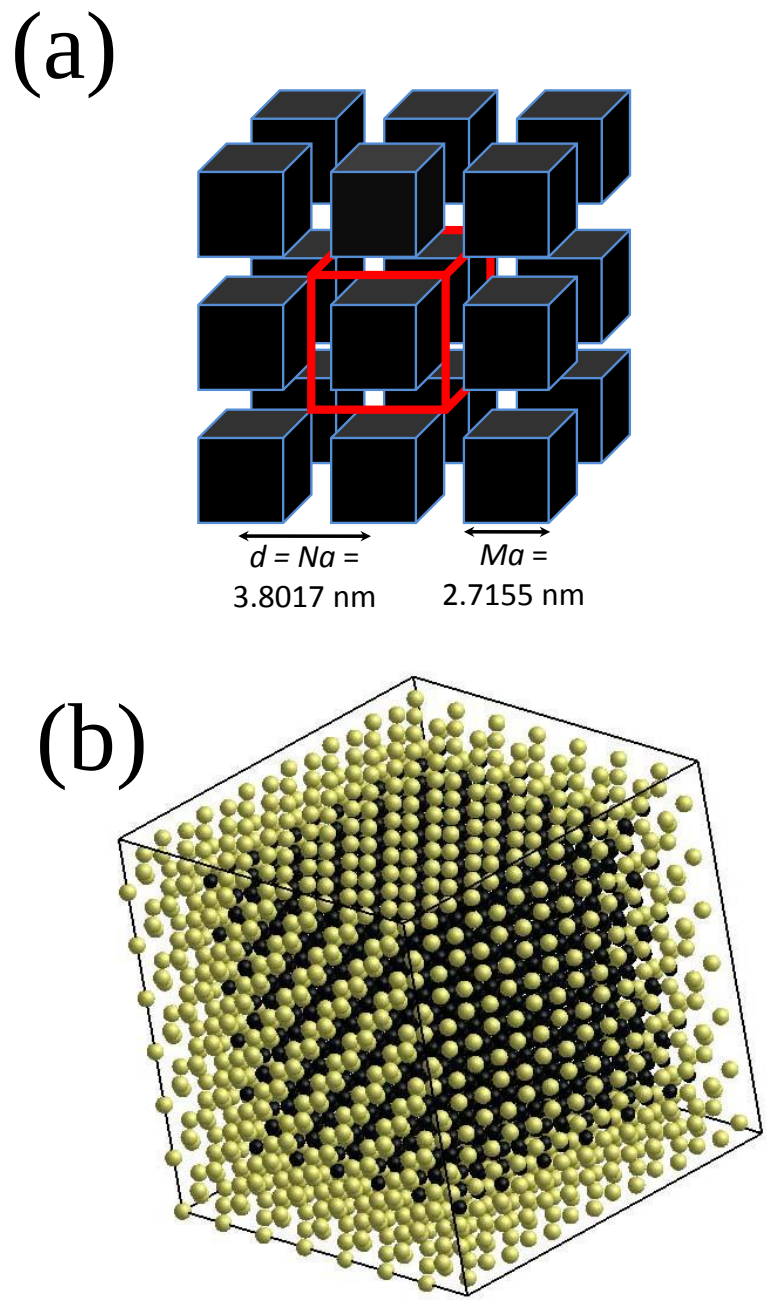

Fig. 1. (Color online) Schematics at two different scales of an atomic-scale 3D phononic crystal with $N = 7$ and $M = 5$. In the continuous medium-like drawing in (a), the quantum dots (QDs) with an edge length of $w = 5a = 2.7155$ nm and spacing of $d = 7a = 3.8017$ nm are displayed by ordered dark (black) cubes with highlighted (blue) edges. In (a), the transparent central cube with thick light (red) edges shows one of the nanomaterial supercells. The discrete medium-like drawing of a supercell is presented in (b). The 1332 Ge atoms forming a QD with a box-like nanoparticle shape in (a) are in dark (black) color in (b) while the 1412 peripheral Si atoms are in light (yellow) color in the remaining of the supercell.

In this case (N = 7, M = 5), each supercell is composed, at its center, of a dc Ge QD composed of M^3 = 125 primitive dc Ge cells. They are surrounded by N^3 - M^3 = 218 peripheral dc Si cells, as in the discrete-medium scheme of Fig. 1(b). In this figure, the Ge and Si atom locations in the supercell are in dark (black) and light (yellow) colors, respectively. The periodic spatial repetition of supercells creates an atomic-scale 3D phononic crystal, as in the continuous-medium scheme of Fig. 1(a). The overall chemical compositions Ge_xSi_{1-x} of the five QD supercrystal configurations with the reduced supercell lattice constant N = 7 are obtained from the Ge-QD filling ratios x = 1.02, 4.59, 12.53, 26.60 and 48.54 Ge at% for the reduced QD bases M = 1, 2, 3, 4 and 5, respectively. As shown in Figs. 1(a) and 1(b), the 3D QD supercrystal shows two scales of crystallinity (i.e. a double crystallinity): The first scale is defined by the inter-atomic distance a between the primitive atoms forming a supercell while the second larger scale is given by the distance $d = Na$ between the Ge QDs.

Since $N_m = 3 \times 8 \times N^3 = 8232$ is the number of vibration degrees of freedom in a supercell with the reduced supercrystal lattice constant N = 7, lattice dynamics is used to compute the 8232 dispersion curves of the five Si/Ge QD supercrystals with N = 7 from their N_m phonon eigenmodes [13]. The empirical Stillinger-Weber potential is preferred to describe the binding energy between two and three neighbor atoms [14,15]. The equilibrium relaxed positions of the atoms in each supercell as a function of the masses and elastic constants of dc Si and Ge are obtained by numerical optimization before lattice dynamics. Since the dispersive effect of each atom in a supercell is considered in this discrete model, the supercrystal dispersion curves are obtained in the THz frequency range. Fig. 2 shows 102 of the 8232 computed dispersions curves of an atomic-scale 3D phononic crystal with the size parameters N = 7 and M = 5 (sketched in Fig. 1). The $N^3 - 3$ = 8229 folded "optical" curves are usually very flat. This harmonic phenomenon results in very low group velocities since they are obtained by derivation of the dispersion branches with respect to the wave number in

a particular direction. The low group velocities constitute a first effect on the extreme thermal-conductivity decrease observed in the Si/Ge QD supercrystals, as explained in the following.

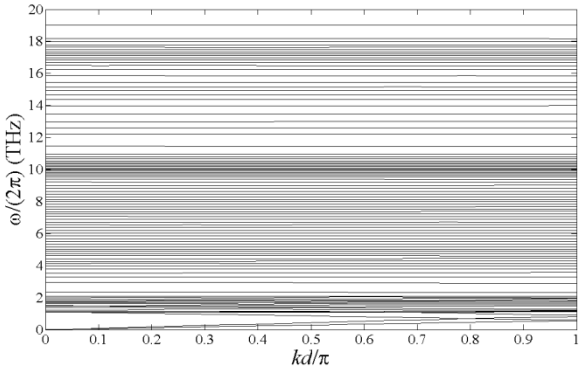

Fig. 2. 102 branches chosen among the 8232 dispersion curves of an atomic-scale 3-D phononic crystal with M = 5 and N = 7 (d = 3.8017 nm); Equivalent crystallographic directions <100>.

B. Thermal Conductivity Model

Using the below general integration [Eq. 1] over the radial wave number $k = |\mathbf{k}|$, as demonstrated in Ref. [11] without using the Debye approximation, we derive the thermal conductivity λ of a 3D crystalline material with a cubic symmetry from its phonon scattering relaxation times $\tau_{k,m}$ and dispersion curves, computed with lattice dynamics (Subsection IIA):

$$\lambda = \frac{1}{3}\sum_{m=1}^{N_m}\int_0^{k_{\max}} \tau_{k,m}(v_{k,m})^2 \hbar\omega_{k,m}\frac{\partial n_{k,m}^{(0)}(T)}{\partial T} g_k \, dk. \qquad (1)$$

In Eq. (1), $\hbar = h/(2\pi)$ is the reduced Planck constant, and m is the index of one branch of the N_m dispersion curves to which belongs the mode (k, m). We remind that the number of eigenvalues is given by $N_m = 24\ N^3 = 8232$ for an atomic-scale 3D phononic crystal with the reduced supercrystal lattice constant $N = 7$. The Bose-Einstein distribution of the phonons is denoted $n_{k,m}^{(0)}(T)$ in Eq. (1) for an equilibrium temperature T. The radial group velocities $v_{k,m} = \partial\omega_{k,m}/\partial k$ [Eq. (1)] are obtained by derivation of the dispersion curves with respect to k. We also point out that the phonon MFPs $l_{k,m}$ can be derived from $l_{k,m} = \tau_{k,m} v_{k,m}$. In Eq. (1), g_k is the free-particle density of states (DOS) per volume unit as a function of k. The integral [Eq. (1)] is taken over the finite interval [0, k_{max}], where k_{max} is the right border of the first folded Brillouin zone (BZ). For a bulk face-centered cubic (fcc) material, this boundary is given by $k_{max} = 2\pi / a$ with the lattice constant a = 0.5431 nm for bulk dc Si. Differently, owing to the sc crystallinity at the largest scale of the Ge QDs, $k_{max} = \pi / d$ is used in Eq. (1) to obtain the thermal conductivity λ of a Si/Ge QD supercrystal with the average distance $d = Na$ between the QDs. In the example of Fig. 1, for a reduced supercrystal lattice constant $N = 7$, the width of the folded BZ is only $1/(2N) = 1/14$ of that of bulk dc Si since $(2\pi / a) / (\pi / d) = 2d / a = 2N = 14$.

C. ***Shrunk Relaxation Times from Incoherent Scattering***

To compute the thermal conductivity λ of the atomic-scale 3D phononic crystal [Eq. (1)], an analytical model of the total phonon relaxation times $\tau_{k,m} = l_{k,m} / v_{k,m}$ of the modes (k, m) is implemented from the Matthiessen rule and scattering cross sections in a "phonon-particle" approach. Only incoherent scattering processes have to be considered. Indeed, the $N^3 - 3$ folded dispersion curves, for which the scattering cross sections are the largest, have folded phonon wavelengths smaller than the double supercell period $2d$. As a result, the (non-

normalized) overall scattering probability $1/\tau_{k,m}$ can be defined from the Mathieussen rule as a summation of two incoherent scattering probabilities:

$$\frac{1}{\tau_{k,m}} = \frac{1}{\tau_{k,m}^{(u)}} + \frac{1}{\tau_{k,m}^{(p)}}. \tag{2}$$

In Eq. (2), the contribution $1/\tau_{k,m}^{(d)}$ of isotopes and atomic-size defects can be neglected. Indeed, this term is a second-order effect in high-purity dc Si. To compute the scattering probability $1/\tau_{k,m}^{(u)}$ of the umklapp (or U) process, a common formulation given in Refs. [19-20], depending on *T*, is utilized. From the precedent, the free-particle DOS per volume unit [Eq. (1)] is defined as $g_k = k^2/\pi^2$ instead of $k^2/(2\pi^2)$ in bulk dc Si with 6 dispersion curves, as discussed in Ref. [11]. In Eq. (2), the multiple-scattering probability $1/\tau_{k,m}^{(p)}$ between the Ge QDs is an incoherent effect resulting from non-focusing and localization of the phonons with small wavelengths and group velocities.

Solving this multiple-scattering problem is highly computationally demanding in three dimensions. An approximated method to obtain $1/\tau_{k,m}^{(p)}$ [Eq. (2)] from the scattering cross section $\sigma_{k,m}^{(p)}$ vs. (*k*, *m*) has to be used. The quantum perturbation approach of Kim and Majumdar [16] is chosen in this study to obtain an approximated analytical model $\sigma_{k,m}^{(p')}$ of the cross sections $\sigma_{k,m}^{(p)}$ of the scatters (i.e. the Ge QDs). This method considers individually each scatter in the framework of the Born approximation when their cross sections remain smaller than the van de Hulst's geometrical limit $2\pi\overline{R}^2$ with the scatter average radius $\overline{R}$. Therefore, owing to BZ folding, the scatter cross sections $\sigma_{k,m}^{(p')}$ of the $N^3 - 3$ folded "optical" modes are assigned in this paper to the same analytical formulations $\sigma_{k,m}^{(ac)} \equiv \sigma_{k,m}^{(p')}$, with m = 1 to 3, than

those of the 3 non-folded "acoustical" modes. This acoustic-like approach leads to an underestimate $\sigma_{k,m}^{(ac)} < \sigma_{k,m}^{(p')}$ of the scatter cross sections. Indeed, the quantity $\sigma_{k,m}^{(ac)}$ is computed in the first half BZ and related to scattering of the 3 non-folded "acoustical" modes. Nevertheless, this approximation enables us to compute an upper limit $\lambda_{max} > \lambda_{real}$ of the thermal conductivity λ of the 3D Si/Ge QD supercrystal. Indeed, the relaxation times $\tau_{k,m}^{(p)}$ [Eq. (2)] are set to the overestimated values given by $\tau_{k,m}^{(ac)}$. As a result, the quantity λ in Eq. (1) is maximized from the inequality $\tau_{k,m}^{(ac)} > \tau_{k,m}^{(p')}$ that holds for any mode (*k*, *m*) since

$$1/\tau_{k,m}^{(ac)} = \eta\sigma_{k,m}^{(ac)}v_{k,m} \text{ and } 1/\tau_{k,m}^{(p')} = \eta\sigma_{k,m}^{(p')}v_{k,m} \text{ leading to } \tau_{k,m}^{(ac)} > \tau_{k,m}^{(p')}, \qquad \text{Eq. (3)}$$

where $\eta = 1/d^3$ is the QD volumic density in [m^{-3}] in the supercrystal [11].

The quantity $\sigma_k^{(p')}$, when taken as a function of only *k*, connects the Rayleigh-type far-field ($\sigma_k^{(F\,Field)}$) and van de Hulst-type near-field ($\sigma_k^{(N\,Field)}$) cross sections arising when $k \to 0$ and $k \to \infty$, respectively, with the following harmonic interpolation:

$$\frac{1}{\sigma_k^{(p')}} = \frac{1}{\sigma_k^{(F\,Field)}} + \frac{1}{\sigma_k^{(N\,Field)}}, \qquad \text{Eq. (4)}$$

where $\sigma_k^{(F\,Field)}$ and $\sigma_k^{(N\,Field)}$ are given in Ref. [16]. These terms depend on the atomic mass *A* and elastic constant *K* of the matrix in which is embedded the scatter with *A* and *K* that differ from those of the matrix by the quantities ΔA and ΔK, respectively [11]. In Eq. (4), the fourth-power dependence of the Rayleigh-type cross section $\sigma_k^{(F\,Field)} \sim \chi^4$ is find back when $k \to 0$, where $\chi = k\overline{R}$ is the average scatter size parameter. Moreover, the near geometrical

cross section $\sigma_k^{(N\,Field)}$ tends to the constant $2G = 2\pi\overline{R}^2$, when $k \to \infty$. This constant is equal to the double of the projected scatter area G according to the extinction paradox [17,18]. From the precedent, an overestimate λ_{max} of the thermal conductivity is computed. Only the acoustic-like part $\sigma_{k,m}^{(ac)}$ of $\sigma_{k,m}^{(p')}$ in Eq. (4) has to be calculated in the first half BZ to obtain $\tau_{k,m}^{(ac)} > \tau_{k,m}^{(p')}$ for any mode (k, m). As a result, in accordance with the analytical developments in Ref. [16], the proportionality factor k^4 in $\sigma_k^{(F\,Field)}$ [Eq. (4)] can be substituted by $(\omega_{k,m} / v_{k,m})^4$ while $\sigma_k^{(N\,Field)}$ is not related to the Debye approximation, as derived in Ref. [11]. This substitution leads to scatter cross sections $\sigma_{k,m}^{(p')} \equiv \sigma_{k,m}^{(ac)}$ and relaxation times $\tau_{k,m}^{(p')} \equiv \tau_{k,m}^{(ac)}$ in Eq. (4) showing a full modal dependency on both k and m and avoids underestimation of λ in Eq. (1). From our calculations, expect at low frequencies for the modes that are not related to thermal transport in solids, a strong predominance of $\sigma_k^{(N\,Field)}$ over $\sigma_k^{(F\,Field)}$ is observed. We obtain $\sigma_{k,m}^{(N\,Field)} >> \sigma_{k,m}^{(F\,Field)}$ for k-values that are already below the middle location of the first folded BZ with $k = \pi / (2d)$ where $\sigma_{k,m}^{(p')}$ is small [11]. Predominance of the near-field effect is consistent with the incoherent scattering model used in this paper.

III. NUMERICAL RESULTS

A. Increasing filling ratio *x* for a constant QD average distance *d*

As detailed in Section II, an upper limit λ_{max} of the thermal conductivity λ is computed as a function of the equilibrium temperature T. Indeed, an incoherent approach is used to obtain the scattering cross sections. This approximation also leads to an overestimate $<l(T)>_{max}$ of the effective phonon MFP. In contrast, the predicted effective product $<(Cv)(T)>$

of the mode heat capacities by their group velocities is not maximized. Indeed, the latter is independent of the phonon relaxation times as given by the following relationships:

$$\lambda(T) = \frac{1}{3}\langle l(T)\rangle\langle (Cv)(T)\rangle \text{ with } \langle Cv(T)\rangle = \sum_{m=1}^{N_m}\int_0^{k_{max}} |v_{k,m}|\hbar\omega_{k,m}\frac{\partial n_{k,m}^{(0)}(T)}{\partial T}g_k dk\,. \quad \text{Eq. (5)}$$

From the formulations of $<Cv>$ [Eq. (5)] and $\lambda(T)$ [Eq. (1)], $<l>_{max}$ is computed as

$$\langle l(T)\rangle = \frac{3\lambda(T)}{\langle (Cv)(T)\rangle}, \quad \text{Eq. (6)}$$

where $<l(T)>$ is maximized for all T-values using the incoherent scattering approach presented in Subsection IIC for the relaxation times.

The dashed-dotted, dashed and solid dark (black) curves from the top to the bottom in Fig. 3(a) present three computed thermal-conductivity curves of λ_{max} with respect to the equilibrium temperature T. They are obtained for three different types of atomic-scale 3D phononic crystals with a constant reduced supercell parameter $N = 7$. However, they show variable odd values of the reduced QD basis M and correspond to the smallest ($M = 1$), middle ($M = 3$) and largest ($M = 5$) QD sizes, respectively. The λ_{max} vs. T curves of two other Si/Ge supercrystal types with the same constant $N = 7$ are displayed using dashed-dotted and dashed light (grey) curves from the top to the bottom in Fig. 3(a). These nanomaterials have even M-values given by $M = 2$ and $M = 4$, respectively. The (red) circles (joined by a dashed curve with the same light color) denote experimental measurements of the thermal conductivity of bulk dc Si in Ref. [20] for comparison. The light (blue) dashed horizontal line [Fig. 3(a)] is a reference to the extreme low limit of amorphous bulk Si with an asymptotical value around 1 W/mK when $T \geq 300$ K according to the Einstein model in Ref. [12]. From the same figure,

the reader can observe the strongest λ decrease for the Si/Ge QD supercrystal with the largest QD filling ratio x = 48.5 Ge at% related to the model parameter M = 5. The latter shows a thermal conductivity that can be lower than λ_{max} = 0.2 W/m/K at T = 300 K.

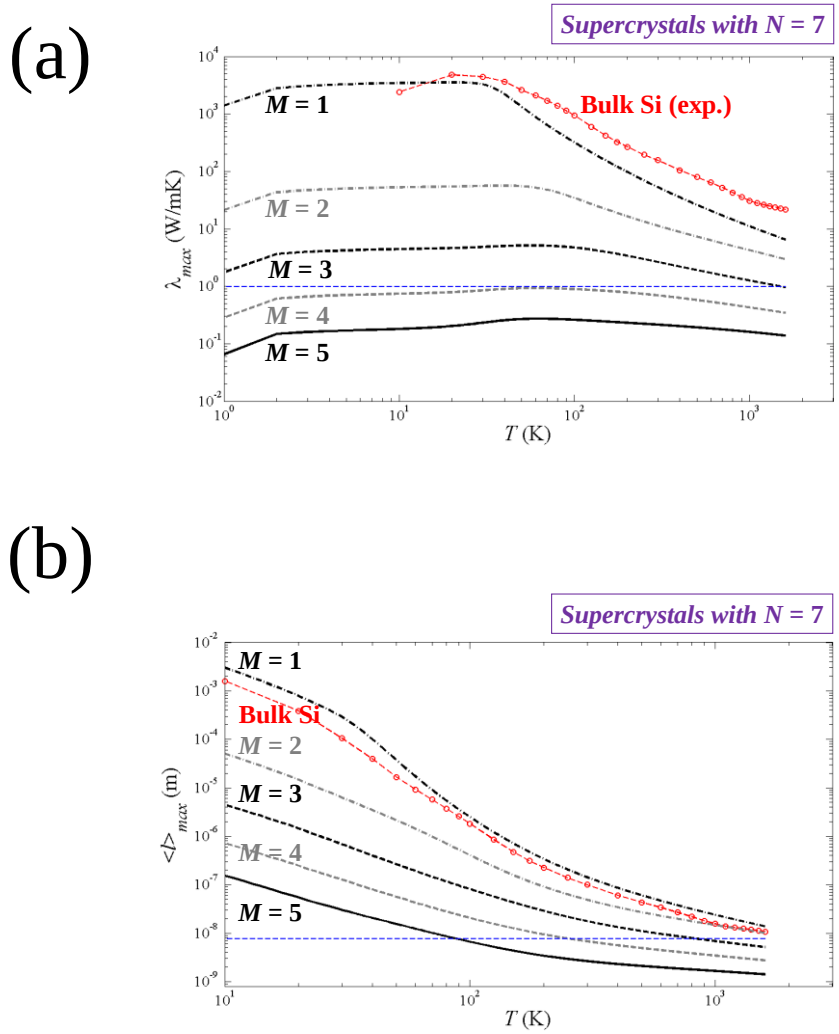

Fig. 3. (Color online) (a) Maximized thermal conductivity λ_{max} vs. T for five atomic-scale 3-D phononic crystals with N = 7: From the top to the bottom, the three dark (black) curves displayed by the dashed-dotted, dashed and solid lines are for odd M-values (M = 1, M = 3 and M = 5, respectively). The two light (gray) curves shown by the dashed-dotted and dashed lines are for even M-values (M = 2 and 4, respectively). The light (blue) dashed horizontal line in (a) is a reference to the Einstein limit (of the amorphous Si thermal conductivity). Circles, joined by the light (red) dashed line are experimental measurements of the bulk dc Si thermal conductivity vs. T. (b) Maximized effective MFP curves $< l >_{max}$ vs. T are displayed by the dashed-dotted, dashed and solid dark (black) lines for odd M-values (M = 1, M = 3 and M = 5, respectively) from the top to the bottom. The two light (gray) curves shown by the dashed-dotted and dashed lines are for even M-values (M = 2 and M = 4, respectively). Circles, joined by the light (red) dashed line give the bulk dc Si effective MFP vs. T. The light (blue) dashed horizontal line in (b) is a reference to the minimal unfolded phonon wavelength of $2d$ = 7.6034 nm when N = 7 for comparison.

This value is 5 folds smaller than the extreme amorphous Si limit and 750 folds smaller than the experimental thermal conductivity (150 W/m/K) of bulk dc Si at room temperature. This amorphous limit is also beaten by another Si/Ge QD supercrystal with a lower filling ratio x = 26.5 Ge at% or M = 4, as shown by the light (gray) dashed curve in the bottom of Fig. 3(a). The latter presents $\lambda_{\max}$ = 0.7 W/m/K at T = 300 K. In contrast, when x = 12.5 Ge at% (i.e. M = 3) and below this value, λ_{max} vs. T is above 1 W/m/K from low to usual operation temperatures of thermoelectric devices [superior part of Fig. 3(a)]. In fact, incoherent scattering becomes less significant when the Ge QDs are smaller and the phonon group velocities increase as well. Fig. 3(a) also shows in the top part that the slope the thermal conductivity of bulk dc Si vs. T is larger than those of the Si/Ge QD supercrystals when T is below 20 K. Indeed, boundary scattering becomes predominant owing to the quite large MFP of bulk dc Si.

Fig. 3(b) shows the five curves of the maximized effective MFPs $<l>_{max}$ with respect to T [Eq. (6)]. This figure has to be matched up with Fig. 3(a). The same conventions of color and hatching than those utilized in Fig. 3(a) are used in the latter figure to relate the five example Si/Ge QD supercrystals with M = 1 to 5 (and constant N = 7). A monotonic decrease of $<l>_{max}$ vs. T can be seen for all examples owing to umklapp scattering [Fig. 3(b)]. Moreover, in the bottom part, significant incoherent scattering is observed from the $<l>_{max}$ dependence of the two QD supercrystals with the largest QD filling ratios x = 26.5 Ge at% (M = 4) and x = 48.5 Ge at% (M = 5), which were also highlighted for the thermal conductivity [Fig. 3(a)]. For these two supercrystals, $<l>_{max}$ becomes lower than the shortest unfolded phonon wavelength of $2d$ = 7.6034 nm, referenced by the light (blue) horizontal dashed line, when $T \geq$ 300 K and $T \geq$ 100 K, respectively [Fig. 3(b)]. These results are in agreement with the utilized incoherent scattering model (Subsection IIC).

B. Increasing QD average distance *d* for a constant filling ratio *x*

In this final discussion, an extreme reduction of the thermal conductivity λ until 0.04 W/m/K is predicted at T = 300 K. This extremely small value, which is lower than twice the thermal conductivity of air, can be obtained for different couples of the size parameters d and x in the Si/Ge QD supercrystal (related to N and M / N in reduced values, respectively). This prediction might have a significant impact on thermoelectrics. Indeed, ZT depends on $1/\lambda$ (Section I). The following results can be extended over a wide temperature range using the T-dependent model described in the precedent.

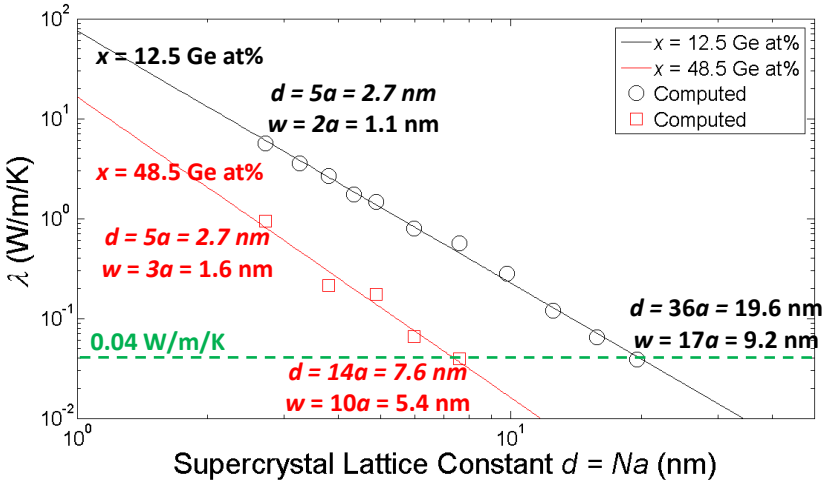

Fig. 4. (Color online) (a) Thermal conductivity λ vs. average distance $d = Na$ between the quantum dots (QDs) for two sets of supercrystals with non-variable Ge filling rations x (related to the M / N ratio) at T = 300 K: The power-law curves of λ vs. d in dark (black) and light (red) colors are obtained for x = 12.5 Ge at% and x = 48.5 Ge at%, respectively. They are the respective interpolations of the computed data denoted by squares and circles for Si/Ge QD supercrystals with the corresponding x = 12.5 Ge at% and x = 48.5 Ge at%.

As shown in Fig. (4), at room temperature $T = 300\ K$, λ shows a power-law decrease for an increasing QD average distance given by $d = Na$ (Subsection IIA) in the 3D Si/Ge supercrystal. Two example curves in dark (black) and light (red) colors are displayed for corresponding chosen x-values of 12.5 Ge at% and 48.5 Ge at% (functions of the ratio M / N). The two λ vs. d curves, plotted with respect to a double-log scale, are obtained by linear interpolations of computed λ-values using the presented model. They are denoted by circles and squares for x = 12.5 Ge at% and x = 48.5 Ge at%, respectively [Fig. 4]. For the largest x = 48.5 Ge at% (squares), λ already reaches the value of 0.04 W/m/K for an average QD distance $d = Na$ = 7.6 nm (i.e. N = 14 in number of inter-atomic distances). This d-value corresponds to an average Ge-QD basis $w = Ma$ = 5.4 nm (i.e. M = 10). However, for the lowest x = 12.5 Ge at% (circles), d has to increase up to 19.6 nm (i.e. N = 36) in order to decrease λ down to the same 0.04 W/m/K value. The latter (d = 19.6 nm, x = 48.5 Ge at %) doublet is related to the average Ge-QD basis w = 9.2 nm (i.e. M = 17). This result gives a good trend for a forthcoming fabrication of a Si/Ge QD supercrystal using the same order of magnitude for the parameters (d, x) as well as current technologies.

The computed thermal conductivity of 0.04 W/m/K shows an agreement with experimental results obtained in Ref. [6] for disordered 2D WSe_2 layered crystals. Owing to double-scale crystallinity in the three spatial dimensions of the Si/Ge QD supercrystal (with folded wavelengths smaller than the double distance 2d), the phonons are trapped between the Ge QDs. This phenomenon is a consequence of significant non-focusing and localization effects as obtained with the proposed model. Similar effects were experimentally observed in the W/WSe_2 system by Chiritescu et al. [6]. When disordering in the W/WSe_2 superlattice to form 2D layered crystal pieces is significantly increased (from large ion doses), their nanomaterial becomes almost amorphous. Therefore, new random thermal paths are generated and the thermal conductivity increases with respect to the supercrystal case [6].

Our theoretical research also shows (from the examples of the Si/Ge QD supercrystal) that an extreme reduction of the thermal conductivity could be obtained independently of the chemical composition of the semiconductor pair used to design a supercrystal with double-scale crystallinity.

IV. CONCLUSIONS

An extreme reduction of the thermal conductivity λ of 3D silicon-based supercrystals with SA Ge QDs is shown from an atomic-scale 3D phononic crystal model. Significant size and temperature effects on the λ-values are discussed. One of the most remarkable result concerns the thermal-conductivity lowering down to only 0.04 W/m/K at room temperature. Such an ultra-low thermal conductivity is computed with size parameters of the 3D Si/Ge supercrystal in the range of the current fabrication technologies, which might present a significant interest for the design of very efficient thermoelectric devices. This theoretical study can be extended to a wide temperature range and is in agreement with experimental results obtained for disordered 2D W/WSe_2 layered crystals [6]. Finally, the modeled extreme thermal-conductivity reduction is expected to be a general property of double-scale crystallinity in 3D QD supercrystals, independently of the semiconductor pair used for their design.

REFERENCES

1. W. Kim, J. Zide, A. Gossard, D. Klenov, S. Stemmer, A. Shakouri, and A. Majumdar, Phys. Rev. Lett. **96**, 045901 (2006).
2. T. M. Tritt, H. Bottner, and L. Chen, Mater. Res. Soc. **33**, 366-368 (2008).
3. A. I. Hochbaum, R. Chen, R. D. Delgado, W. Liang, E. C. Garnett, M. Najarian, A. Majumdar, and P. Yang, Nature **451**, 163-167 (2008).
4. A. I. Boukai, Y. Bunimovich, J. Tahir-Kheli, J.-K. Yu, W. A. Goddard III, and J. R. Heath, Nature **451**, 168-171 (2008).
5. S. Volz, and G. Chen, Appl. Phys. Lett. **75**, 2056-2058 (1999).
6. C. Chiritescu, D. G. Cahill, N. Nguyen, D. Johnson, A. Bodapati, P. Keblinski, and P. Zschack, Science **315**, 351-353 (2007).
7. K. F. Hsu, S. Loo, F. Guo, W. Chen, J. S. Dyck, C. Uher, T. Hogan, E. K. Polychroniadis, and M. G. Kanatzidis, Science **303**, 818-821 (2004).
8. T. C. Harman, P. J. Taylor, M. P. Walsh, and B. E. LaForge, Science **297**, 2229-2232 (2002).
9. R. Venkatasubramanian, E. Siivola, T. Colpitts, and B. O'Quinn, Nature **413**, 597-602 (2001).
10. See references in *Nanoscale Heat Transport - From Fundamentals to Devices*, R. Venkatasubramanian, Ed. (Mater. Res. Soc. Symp. Proc. Volume 1172E, Warrendale, PA, 2009).
11. J.-N. Gillet, Y. Chalopin, and S. Volz, ASME J. Heat Transfer **131**, 043206 (2009).
12. D. G. Cahill, S. K. Watson, and R. O. Pohl, Phys. Rev. B **46**, 6131-6140 (1992).
13. M. T. Dove, *Introduction to Lattice Dynamics*, Cambridge Topics in Mineral Physics and Chemistry, No 4 (Cambridge Univ. Press, Cambridge, UK, 1993).
14. Z. Jian, Z. Kaiming, and X. Xide, Phys. Rev. B **41**, 12915-12918 (1990).
15. Y. Chalopin, J.-N. Gillet, and S. Volz, Phys. Rev. B **77**, 233309 (2008).
16. W. Kim, and A. Majumdar, J. Appl. Phys. **99**, 084306 (2006).
17. C. F. Bohren, and D. R. Huffman, *Absorption and Scattering of Light by Small Particles* (Wiley, New York, 1998).
18. H. C. van de Hulst, *Light Scattering by Small Particles* (Dover, New York, 1981).
19. C. J. Glassbrenner, and G. A. Slack, Phys. Rev. **134**, A1058-A1069 (1964).
20. G. A. Slack, and S. Galginaitis, Phys. Rev. **133**, A253-A268 (1964).